

SYNCHRONOUS OPTICAL AND ELECTRICAL PD MEASUREMENTS

S. Behrend^{1*}, W. Kalkner¹, G. Heidmann², H. Emanuel³, R. Plath⁴

¹ High Voltage Engineering, Technical University Berlin, Germany, ²IPH Berlin, Germany, ³OMICRON mtronix, Germany, ⁴HPS Berlin, Germany

*Email: sbehrend@mailbox.tu-berlin.de

Abstract: Sensitive partial discharge (PD) measurements on HV/EHV cable systems are usually based on electrical or electromagnetic PD detection. Unfortunately, interferences may significantly reduce sensitivity, especially in on-site after installation testing. This paper deals with optical PD detection which is absolutely immune to any kind of electromagnetic interferences. In this paper, we report on investigations on transparent silicone probes with artificial PD defects. Measurements were performed with a specialized PD measuring system with synchronous optical and electrical channels. Results show a clear correlation in between optical intensity and electrical discharge magnitude.

1 INTRODUCTION

The measurement of partial discharges (PD) is an approved diagnostic method for insulation condition assessment, able to detect even very small defects. Consequently, electrical PD measurements according to IEC 60270 entered the relevant product standards and became an integral part of routine testing of almost all types of high voltage equipment. PD measurements in accordance with IEC 60270 are so-called *conventional*.

Conventional PD measurements are sensitive to noise, raising the need for screened test chambers, line filters and PD-free HV test equipment.

In contrast, on-site PD measurements are exposed to noise. So-called non-conventional PD detection, e.g. electromagnetic, acoustic and optical PD detection, offers alternatives for sensitive and selective PD detection under noisy conditions [1-3]. An overview about the increasing use of fibre optical sensors in high voltage facilities is given in [4].

Optical PD detection is restricted to transparent or translucent insulation materials. Therefore the major application is detection and (inherently) location of corona or surface discharges in air.

Besides, optical PD detection was applied to scaled down models of GIS and offered several advantages over electrical PD detection techniques [3]. It was more sensitive, had a higher signal-to-noise ratio and could detect glow (pulseless) discharges.

Electromagnetic immunity is another important advantage of optical over electrical PD detection when measuring PD during impulse voltage stress.

Similar to GIS, cable terminations and joints also operate in a light-tight enclosure, excluding any impact of ambient light. Using transparent or translucent stress-cone materials and new high-sensitive optical sensors, noise-immune optical PD detection may become a viable part for insulation condition assessment.

Until now, there has been no extensive use of optical methods in PD detection, especially inside full-sized high voltage equipment. Nevertheless, similar optical systems were very successfully used for measurements in the field of aging of solid polymer insulation materials [5, 6]. First reported results in connection with PD detection in silicone probes and EHV-stress-cones are promising [7]. Further investigation should focus on different types of PD defects and their light-charge-relation.

This paper deals with synchronous optical and electrical PD measurements and presents a short survey on investigation results.

2 TECHNICAL IMPLEMENTATION

2.1 Experimental set-up

The experimental set-up for the optical/electrical PD measurements is shown in Figure 1. It consists of a high-voltage source, a coupling capacitor and the PD measuring system MPD 600 (Omicron) with electrical and optical channels. The PD measuring system consists of synchronous multi-channel PD acquisition, real-time pre-processing hardware, communication via optical fibre, a standard PC for system control and result visualization as well as evaluation according to IEC 60270 [8].

The electrical channel (unit 1.1 Q) is used for conventional PD measurements and consists of a quadripole/measuring impedance (CPL 542) and the partial discharge analysis system (MPD 600).

The main parts of the optical channel unit 1.x Q ($x=2, 3, 4$) are a special type fluorescent fibre sensor (FOF) [9], applied on high voltage potential, together with a glass optical fibre and a special optoelectronic converter (APD 500).

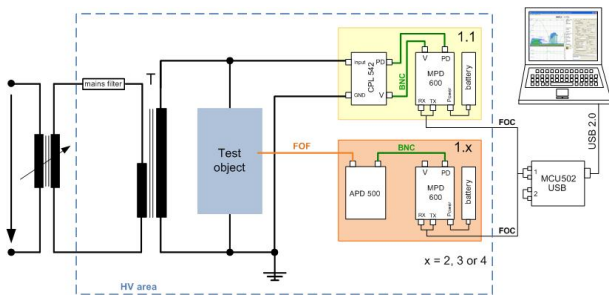


Figure 1 Experimental set-up

The fluorescent optical fibre collects faint light emission from PD's coming from any incident angle and even through the side of the fibre [9].

As long as the wave lengths of the incident light of PD events fall within the absorbed spectrum of the fibre, photons are absorbed and guided to the end of the fluorescent optical fibre and to the connected glass fibre. Its function is the light transport to the converter with low attenuation.

The selected type of sensor should be constructed very robustly to ensure long-term reliable operation also for on-site application [7].

The optoelectronic converter APD500 achieves high sensitivity, dynamic and speed by utilizing an avalanche photodiode with 200 V bias voltage. In general, such converters have to balance bandwidth (pulse resolution time) and Signal to Noise Ratio (SNR). In this case, a bandwidth of 500 kHz was chosen. Each pulse-type light emission of a single PD pulse is converted into an electrical pulse of fixed pulse width and variable pulse magnitude, proportional to the light intensity. Therefore, the electrical output of the APD500 can be directly sent to the input of the MPD600 PD detection unit. Due to the very short delay of the APD500 in between optical input and electrical output (typ. 400 ns) and due to the multi-channel architecture of the MPD600 system it became possible to correlate optical and electrical signals on a pulse-by-pulse base. The APD500 noise level depends directly on the ambient light intensity, requiring best-possible darkness to reach maximum sensitivity.

The signals of electrical and optical channels are transmitted via optical fibres to the control unit (MCU 550) and to the computer.

This measurement system enables data recording and visualization of the electrical and optical impulses with the same software typically used for PD measurements in form of PRPD pattern,

apparent charge and impulse rate. It's important to emphasize that only the electrical channel is calibrated and the apparent charge is given in pC [10].

2.2 Simulated defects

To check the possibilities of an optical PD detection, typical defects in accessories were simulated in different silicone probes and their behaviour was examined in dependence on voltage and time.

Figure 2 shows typical test samples with wrapped fluorescent optical fibres. The defects are simulated by using embedded tip-plane-electrode configurations within specially prepared probes, e.g.:

- **Needle embedded** in a transparent silicone probe (Figure 2 left hand side, simulation of a conductive particle within accessory insulation)
- **Artificial channel** at a needle tip in a transparent silicone probe (Figure 2 right hand side, simulation of a channel with a big length-to-diameter relation (similar to a tree channel) within e.g. an accessory)
- **Needle in the interface XLPE/silicone** of a probe (simulation conductive defect in the interface XLPE/silicone of accessories, Figure 3)

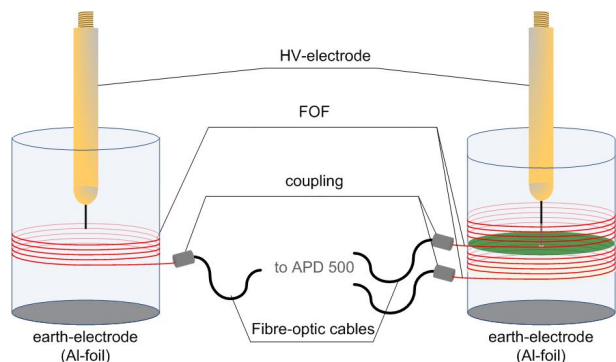


Figure 2 Test samples (schematic) without and with optical dense separation layer (green)

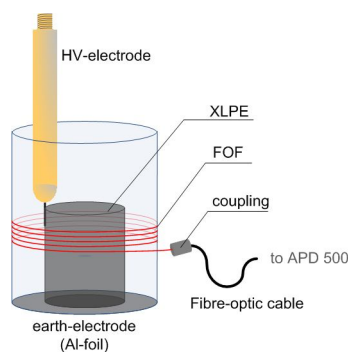


Figure 3 Test samples (schematic) interface XLPE/silicone

- **defect in the interface** cable core/stress cone by using an XLPE cable and a transparent stress cone model (Figure 4). For more details see [7].

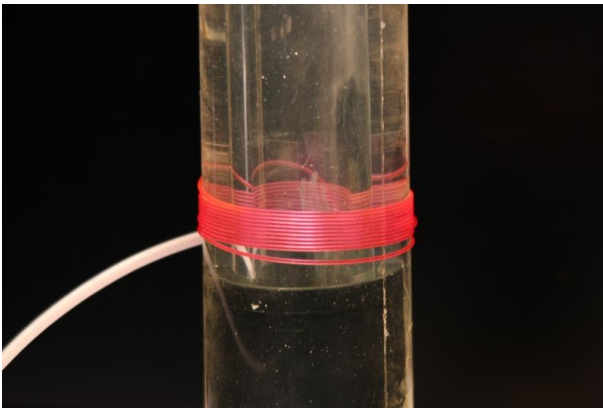


Figure 4: Model of a stress cone with integrated fluorescent optical fibres (parts of the outer cover were removed)

3 RESULTS OF INVESTIGATION

The measurements were carried out in laboratories with and without electromagnetic shielding, always in complete darkness.

Before start of the measurements the electric PD channel was calibrated according to IEC 60270.

In the following survey some typical results are presented:

3.1 PRPD pattern

A comparison of electrical and optical PRPD-patterns for a needle in a silicone probe in Figure 5 shows a nearly identical visualization. The majority of the discharges occur within the first positive and first negative quarter wave of the applied voltage. Such visualization is typical for PDs within a polymeric insulation.

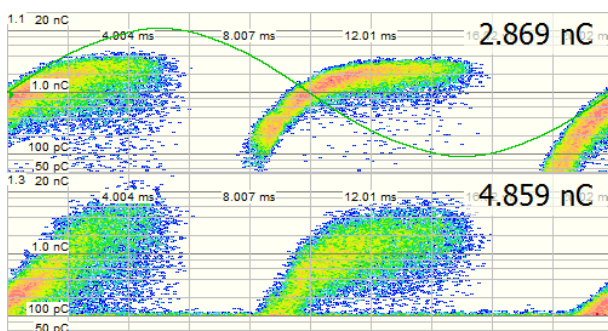


Figure 5: PRPD pattern (electrical channel above, optical channel below), needle tip diameter 1.5µm, AC voltage 22.6kV

Please note that the dimension unit of light intensity (nC/pC) is a result of the measurement software. Only the electrical channel is calibrated. The units of the optical channels are arbitrary units.

PRPD patterns of a probe with an artificial channel at the needle tip are depicted in Figure 6. Because optical pulses can develop in the channel and in a growing tree we use two optical sensors to measure these different discharges (see Figure 2).

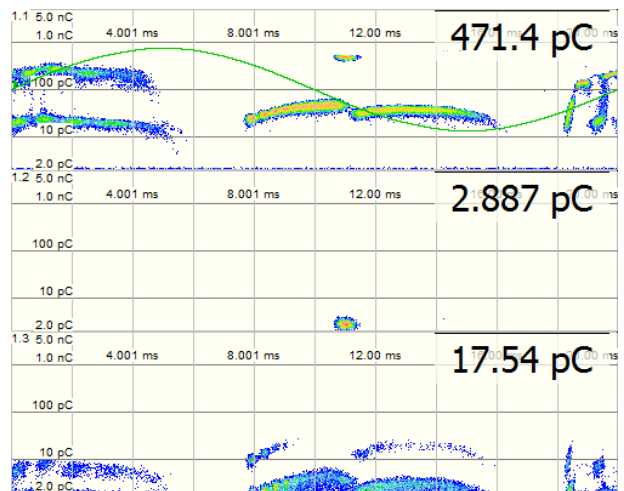


Figure 6: PRPD pattern (electrical channel above, optical channel middle and below), needle tip diameter 3.1µm, AC voltage 7.3kV

In unit 1.1 Q (above) we can discern PDs in the artificial channel and the tree. The first optical unit 1.2 Q (middle) shows the pulses in the tree and the unit 1.3 Q (below) the pulses in the artificial channel. Here the visualization of the two optical channels is similar to the electrical PRPD diagram.

On principle we found the same behaviour also for the other simulated defects.

3.2 POT- diagram

A similar behavior should be appearing in POT (Pulses Over Time) diagrams. In a POT- diagram we compare the values of the electrical and optical impulses in relation to the phase of the voltage in chronological order.

A typical 4-cycle pulse sequence of electrical and optical PDs is shown in Figure 7 for a needle in silicone and in Figure 8 for an artificial channel at the needle tip at a constant AC voltage respectively. The pattern in Figure 7 (unit 1.1 Q) is composed of increased pulses correlating to the increasing phase angle, which is typical for an electrical tree. The diameter of the artificial channel is 150µm. But a simulation of an electrical tree needs a long channel with a very small diameter (e.g. 5 mm length and a diameter of 40 µm [11]).

In the POT-diagram (Figure 8) of an artificial channel at the needle-tip (length/diameter ratio of appr.70) and a growing tree, starting from the tip of the channel, we can see differences in the number of discharges in both optical PD units (unit 1.3 Q and unit 1.4 Q). This is in accordance with the PRPD pattern (not shown).

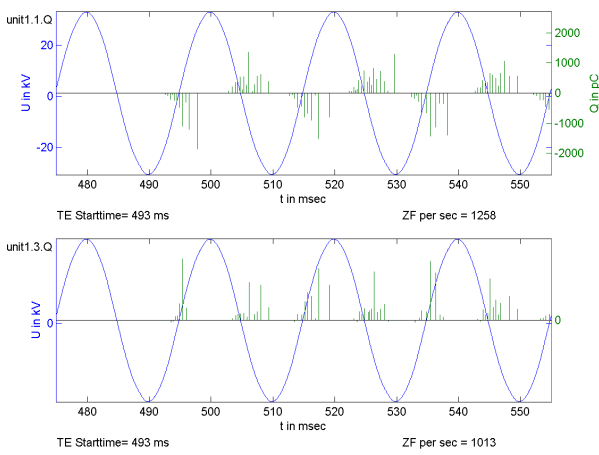


Figure 7: POT-diagram (electrical channel above, optical channel below), needle tip diameter 1.5µm, AC voltage 22.5 kV

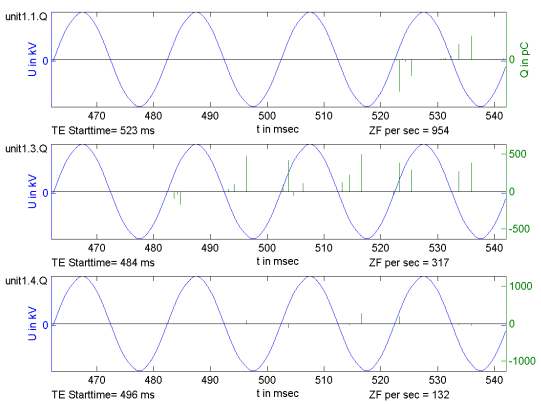


Figure 8: POT-diagram (electrical channel above, optical channel middle and below), needle tip diameter 70µm, channel length 5mm

3.3 Comparison of charges

In Figure 9 the comparison of electrical apparent charge with the optical intensity Q_{opt} is shown for a needle in silicone. The course of both values in dependence on measuring time is very similar. In a rough approximation the light emitted by partial discharges is proportional to their charge [11].

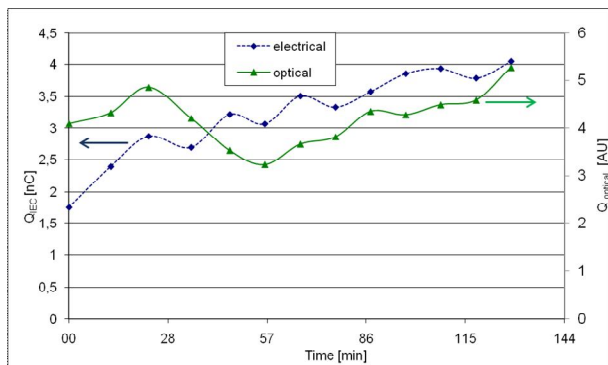


Figure 9: Apparent charge Q_{IEC} and optical intensity Q_{opt} , needle in silicone, needle tip diameter 1.4µm, AC voltage 22.6kV

3.4 Counts per seconds

Similar to measurements with a photomultiplier in a Geiger modus we can also compare the counts per second in the optical and electrical channel. Figure 10 depicts an example together with the apparent charge depending on the voltage. The course is very similar and the number in the optical channel is lower. With the beginning of PD's the counts in both channels begin to rise.

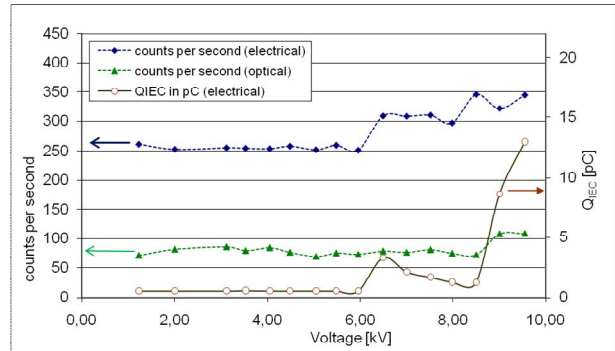


Figure 10: Trend of optical and electrical PD magnitude and apparent charge over AC voltage, needle tip diameter 1.5µm,

3.5 Model stress cone with artificial defect

Additionally a 20-kV-XLPE cable with a transparent model stress/cone (Figure 4) was also examined. The defect in the interface cable-stress cone is a semiconducting tip on earth potential. Supplementary a tip on high voltage in air was used. A comparison of the PRPD patterns of the electrical and optical channels unit 1.1 Q and unit 1.2 Q respectively is depicted in Figure 11. In the picture of the electrical channel we clearly see the PD's resulting from the tip in air. This is also demonstrated in the POT diagram (Figure 12) with the electrical channel (unit 1.1.Q) and the optical channel (unit 1.2.Q). Only in the picture of the electrical channel we see the typical discharges for a tip on HV.

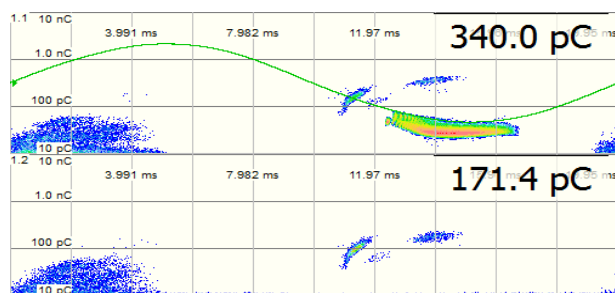


Figure 11: PRPD pattern (electrical channel above, optical channel below), cable and tip in air on high voltage, AC voltage 7.8kV

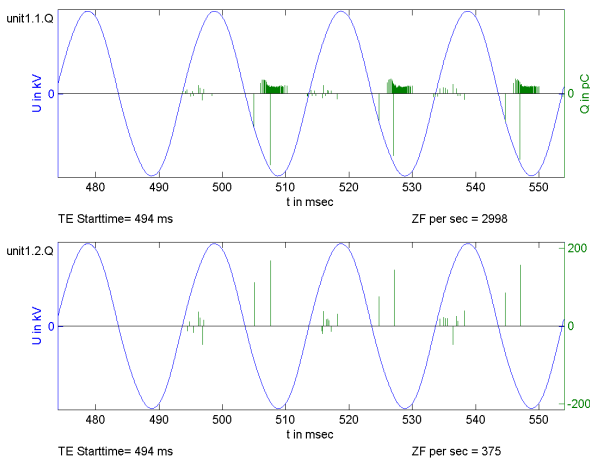


Figure 12: POT-diagram (electrical channel above, optical channel below), cable and tip in air on high voltage, AC voltage 7.8kV

In Figure 13 the electrical and optical PD detection is compared in dependence on voltage. There are depicted the apparent (electrical) charge (Q_{IEC}) and the numbers of electrical and optical pulses within a fixed time range. At low voltages, below the inception voltage for the tip on high voltage in air, the number of detected optical and electrical pulses is similar. When the discharges of the tip on high voltage in air appear, the number of electrical pulses and the apparent charge grow, whereas the number of optical pulses remains nearly constant.

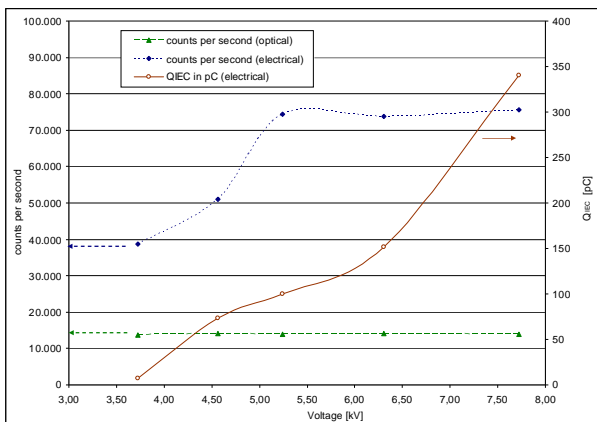


Figure 13: Trend of optical and electrical PD magnitude and apparent charge (stress cone with semiconducting tip and tip on high voltage in air)

The rise of the optical counts is too small to show it in the Figure 13.

4 NEW POSSIBILITIES OF ANALYSIS

4.1 NAR diagram

In a NAR (Normalized Amplitude Relation) diagram the relation between electrical and optical Amplitude is depicted. During an individual measurement with a fixed time range recorded by the MPD-System, the magnitudes of individual optical and electrical pulses are referred to their maximum value (value between 0 and 1). Unit

1.3Q and unit 1.4 Q represent the optical channels and unit 1.1Q the electrical channel.

Figure 14 shows the comparison of electrical and optical events on a pulse-by-pulse basis for a needle in silicone. The correlations of electrical and optical pulses are gathered around the diagonal with a spread scattering region indicating a nearly proportional relation of apparent charge and optical intensity.

The NAR diagrams in Figure 15 and Figure 16 result from measurements of the probe with an artificial channel (electrical tree). Figure 15 shows the correlation in between unit 1.1 Q and unit 1.3 Q (can only detect the optical discharges in the artificial channel) and Figure 16 the correlation with unit 1.4 Q (discharges in the tree, which grows from the tip of the channel (see also Figure 2).

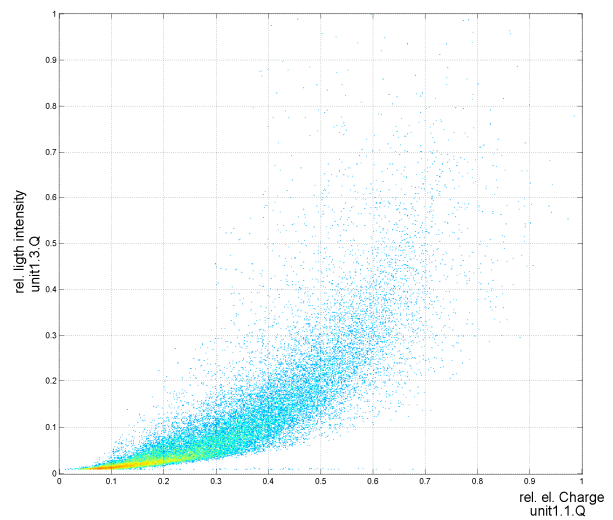


Figure 14: NAR diagram of electrical and optical events, time range 60 μ s, needle tip diameter 9.67 μ m

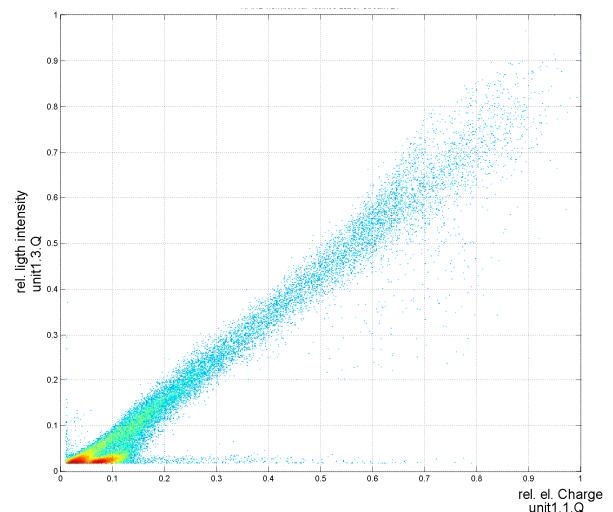


Figure 15: NAR diagram of electrical and optical events, time range 60 μ s, needle tip diameter 70 μ m, channel length 5mm; optical unit detects TE in the channel

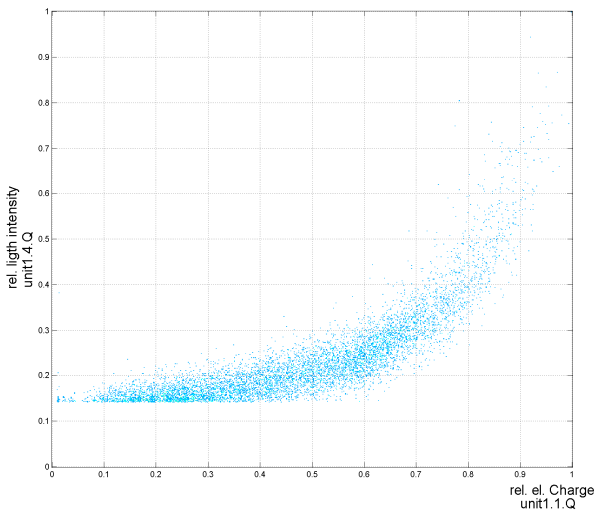


Figure 16: NAR diagram of electrical and optical events, time range 60 μ s, needle tip diameter 70 μ m, channel length 5mm, optical unit detects TE in the growing tree on the tip of the channel

The gathering around the diagonal may be different in dependence on the type of defect.

5 CONCLUSION

Optical PD detection inside of outdoor cable terminations is absolutely immune to any kind of electrical, electromagnetic or acoustic interference.

Optical PD detection using fluorescent fibers is possible and showed high sensitivity on transparent and translucent silicone elastomers, promising similar success in on-site applications.

Synchronous optical and electrical PD detection and pulse-by-pulse correlation enabled direct evaluation of PD light intensity in terms of pC.

Optical PD detection may offer possibilities for localizing PD sources within insulation systems.

Investigations performed until now show possibilities for improved fluorescent optical fibers for an easier integration in e.g. stress-cones, higher sensitivity and robust design together with an improvement of the optical converter. There are also some open questions about the correlation between light intensity and apparent charges for different PD defects in connection with an early detection of optical pulses.

We think an optical detection offers some benefits, alone or together with the electrical PD detection, in the field of PD measuring and insulation monitoring.

6 ACKNOWLEDGMENTS

This work was supported by IBB Investitionsbank Berlin within the ProFIT-program for promotion of

research, innovations and technology under the grant numbers 10134042 till 10134047. This support is much appreciated.

7 REFERENCES

- [1] R. Schwarz, et.al.: Review of Partial Discharge "Monitoring Techniques used in High Voltage Equipment", IEEE 2008 Annual Report Conference on Electrical Insulation Dielectric Phenomena
- [2] D. Zhu; et.al.: "Partial Discharge Detection in cable Termination Using Acoustic Emission Techniques and Adaptive Signal Processing", Conference Record of the 1994 IEEE International Symposium on Electrical Insulation, Pittsburgh, PA, USA, June 5-8; 1994, 74-76
- [3] M. Kaufhold, S. S. Bamji, A.T. Bulinski: Optical Detection of Partial Discharges in Gas-Insulated Systems; 1996 IEEE Annual Report Conference on Electrical Insulation Dielectric Phenomena, San Francisco; October 20-23, 1996, 618-622
- [4] W. Habel; et.al.: „Fibre optical sensors for early damage detection in electrical insulations and mechanical components in high voltage facilities" ISH 2011
- [5] G. Teyssedre; G. Tardien; D. Marcy; C. Laurent: "AC and DC electroluminescence in insulating polymers and implication for electrical ageing", J. Phys. D: Appl. Phys. Vol. 34, 2220-2229, 2001
- [6] J.V. Champion; et.al.: "The correlation between the partial discharge behaviour and the spatial and temporal development of electrical trees grown in an epoxy resin", J. Phys. D: Appl. Phys. Vol. 29, 2689-2695, 1996
- [7] M. Habel; et.al. "Optical PD Detection in stress cones of HV cable accessories" Jicable 2011,
- [8] W. Koltunowicz and R. Plath,: "Synchronous multi-channel PD measurements", IEEE TDEI, Vol. 16, No 6, pp. 1715-1723, 2008
- [9] R. Mangeret; et. al.; "Optical Detection of Partial Discharges using Fluorescent Fiber" IEEE TEI, Vol. 26, No. 4 783-789, 1991
- [10]K. Schon; et.al.: "Typprüfung eines digitalen TE-Messsystems nach IEC60270", 3. ETG-Fachtagung Diagnostik elektrischer Betriebsmittel, Kassel, September 2006
- [11]Kai Wu, et.al.: "A Novel Physical Model for Partial Discharge in Narrow Channels" IEEE TDEI, Vol. 6, No 2, pp 181-190, 1999